Bad-Dependent Rafts Alteration Is a Consequence of an Early Intracellular Signal Triggered by Interleukin-4 Deprivation

Aarne Fleischer,[1] Ata Ghadiri,[1] Frédéric Dessauge,[1] Marianne Duhamel,[1] Xavier Cayla,[3] Alphonse Garcia,[2] and Angelita Rebollo[1]

[1]Laboratoire d'Immunologie Cellulaire et Tissulaire, Institut National de la Sante et de la Recherche Medicale U543, Hôpital Pitié Salpetrière; [2]Unité de Chimie Organique, Institut Pasteur, Paris, France and [3]Equipe Hypophyse, UMR6073 INRA-Centre National de la Recherche Scientifique, Université de Tours, Physiologie de la Reproduction et des Comportements, Nouzilly, France

Abstract

Many molecules are inducibly localized in lipid rafts, and their alteration inhibits early activation events, supporting a critical role for these domains in signaling. Using confocal microscopy and cellular fractionation, we have shown that the pool of Bad, attached to lipid rafts in proliferating cells, is released when cells undergo apoptosis. Kinetic studies indicate that rafts alteration is a consequence of an intracellular signal triggered by interleukin-4 deprivation. Growth factor deprivation in turn induces PP1α phosphatase activation, responsible for cytoplasmic Bad dephosphorylation as well as caspase-9 and caspase-3 activation. Caspases translocate to rafts and induce their modification followed by translocation of Bad from rafts to mitochondria, which correlates with apoptosis. Taken together, our results suggest that alteration of lipid rafts is an early event in the apoptotic cascade indirectly induced by interleukin-4 deprivation via PP1α activation, dephosphorylation of cytoplasmic Bad, and caspase activation. (Mol Cancer Res 2004; 2(12):674–684)

Introduction

Apoptosis is a genetically regulated process that allows removal of abnormal growing cells and controls homeostasis. Apoptosis may be induced by drugs, radiations, infections, or growth factor deprivation as well as by signals transmitted through membrane receptors. Apoptosis eliminates cells in an ordered manner, and deregulation of the apoptotic machinery can lead to many diverse diseases (1-4).

The Bcl-2 family proteins act as a decision point in the apoptotic pathway by regulating the permeabilization of the outer mitochondrial membrane. This family comprises both pro-apoptotic and antiapoptotic members, including the BH3-only member Bad, which promotes apoptosis. Thus far, 10 distinct BH3-only proteins have been described in mammals. The reason for this redundancy remains unexplained. It has been suggested that BH3-only members function as death sensors where various death stimuli seem to activate different BH3-only proteins (5, 6).

The serine/threonine protein phosphatases are usually classified as type 1 (PP1) or type 2 (PP2) depending on their substrate specificity and sensitivity to inhibitors. PP1 and PP2 are abundant serine/threonine phosphatases expressed in mammalian cells (7). PP1 represents a family of holoenzymes generated by specific interactions between catalytic subunits and a wide variety of regulatory or anchoring proteins involved in targeting as well as in controlling phosphatase activity (8, 9). PP2A enzymatic activity is reported to be more potently inhibited by okadaic acid (10, 11), and controlled concentrations of okadaic acid can selectively inhibit PP2A without affecting PP1 activity (12). We have shown that Bad is an *in vitro* and *in vivo* substrate for PP1α and that growth factor deprivation–induced apoptosis operate by regulating cytoplasmic Bad dephosphorylation through PP1α phosphatase (13). We have also shown that growth factor deprivation of TS1αβ cells induces a mitochondrial-mediated apoptotic pathway that leads to cytochrome *c* release, thus activating caspase-9 and caspase-3 (14).

Localization of proteins to distinct subcellular compartments, including membranes, is a critical event in multiple cellular pathways, such as apoptosis. Plasma membranes of many cell types contain microdomains called lipid rafts, which are biochemically different from bulk plasma membrane (15-17). These domains are enriched in sphingolipids and cholesterol and show resistance to Triton X-100 solubilization and can be isolated by density gradient ultracentrifugation. It has also recently been shown using *in vitro* experiments that ceramide lipid, which is involved in important biological processes, reside and function within rafts (18). Rafts may be visualized in intact cells by confocal microscopy using fluorescently labeled cholera toxin subunit B, which binds to the ganglioside GM1 (19).

Many receptors are inducibly localized in lipid rafts, which have been shown to function as platforms coordinating the induction of signaling pathways. Disruption of lipid rafts inhibits early activation events, supporting a critical role for these domains in signaling. Recent publications have proposed that rafts are involved in the control of apoptosis via positive

Received 7/12/04; revised 10/1/04; accepted 11/17/04.
Grant support: Institut Pasteur, Institut National de la Sante et de la Recherche Medicale-Avenir, and Fondation pour la Recherche Médicale.
The costs of publication of this article were defrayed in part by the payment of page charges. This article must therefore be hereby marked advertisement in accordance with 18 U.S.C. Section 1734 solely to indicate this fact.
Requests for reprints: Angelita Rebollo, Laboratoire d'Immunologie Cellulaire et Tissulaire, Institut National de la Sante et de la Recherche Medicale U543, Hôpital Pitié Salpetrière, Bâtiment CERVI, 83, Boulevard de l'Hôpital, 75013 Paris, France. Phone: 33-142177527; Fax: 33-142177490. E-mail: rebollo@chups.jussieu.fr

interactions involving Fas or via negative interactions involving Bad (20-23). It has been shown that interaction of Fas with rafts induces apoptosis in HL-60 and Jurkat cell lines (23), and disruption of membrane rafts integrity inhibits Fas-dependent apoptosis in leukemic cells as well as in cell lines. In addition to Fas, other apoptotic molecules, such as Fas-associated death domain protein, pro-caspase-8, pro-caspase-10, c-Jun NH_2-terminal kinase, and Bid, are recruited into rafts, linking Fas and mitochondria signaling pathways (24). Moreover, caspase-3 is also a component of the Fas-inducing signaling complex in lipid rafts, and its activity is required for caspase-8 activation in Fas-induced cell death (25). This translocation of Fas into rafts may provide a mechanism for amplifying Fas signaling through reorganization of membrane microdomains. In resveratrol-induced apoptosis, Fas is triggered to membrane rafts in SW480 human colon cancer cells together with Fas-associated death domain protein and pro-caspase-8. This redistribution is associated with the formation of the death-inducing signaling complex (26). In addition, Akt2, phosphatidylinositol 3′-kinase, protein kinase C, and PTEN are also localized in lipid rafts (27, 28). In the same direction, recruitment of tumor necrosis factor receptor to rafts is essential for tumor necrosis factor-α–mediated nuclear factor-κB activation (29). Other signaling molecules, such as the Lck kinase and interleukin (IL)-2 and IL-15α subunit receptor, are also associated to lipid rafts (30, 31). The translocation of Lck to rafts regulates Fyn kinase activity. Finally, tyrosine-phosphorylated CD28 is recruited to lipid rafts and is associated to phosphatidylinositol 3′-kinase in both Jurkat and peripheral blood T lymphocytes (32). Bad resides in rafts in proliferating T cell lines and thymocytes while associated to mitochondria in apoptotic cells. Changes of rafts integrity induce segregation of Bad from rafts followed by its translocation to mitochondria, which correlates with apoptosis induction (22, 33). Here, we show that alteration of rafts is a consequence of an intracellular signal initiated by cytoplasmic Bad dephosphorylation and represents an early biochemical hallmark in the apoptotic process induced by IL-4 deprivation.

Results

IL-4 Deprivation Induces Alteration of Lipid Rafts

TS1αβ is a lymphokine-dependent murine T cell line. When IL-4-maintained cells are deprived of lymphokine, they undergo apoptosis (Table 1). As early as 4 hours after IL-4 deprivation, 14% of the cells were apoptotic, progressively increasing and reaching 47% on 24 hours of IL-4 starvation. Control IL-4-stimulated cells showed no significant level of apoptosis.

Given that 4 hours after IL-4 deprivation we already were able to distinguish apoptosis signals, we analyzed whether alteration of rafts was detected on this short period of lymphokine deprivation. For this purpose, IL-4-stimulated or IL-4-deprived cells were incubated with cholera toxin subunit B coupled to FITC, which binds to ganglioside GM1, followed by fluorescence-activated cell sorting analysis. As shown in Fig. 1A, a significant diminution of the signal intensity with the rafts marker cholera toxin-FITC was observed 4 hours after IL-4 deprivation. The level of staining progressively decreases as the IL-4 starvation period increases (Fig. 1A), reaching the minimum level of signal intensity 24 hours after lymphokine withdrawal. Figure 1B illustrates the mean fluorescence of cholera toxin-FITC labeling of control and IL-4-deprived cells. This result suggests an early alteration of rafts on growth factor deprivation that may trigger subsequent apoptotic events.

Table 1. IL-4 Starvation Induces Apoptosis in TS1αβ Cells

Apoptotic Cells (%)		
Time (h)	IL-4	Apoptosis
0	+	5 ± 2
4	–	14 ± 3
8	–	22 ± 2
12	–	30 ± 4
16	–	36 ± 3
24	–	47 ± 5

NOTE: Cells were cultured in the presence or absence of IL-4 for the indicated times, harvested, diluted in ice-cold binding buffer, stained with Annexin and propidium iodide, and analyzed by flow cytometry. Percentages ± SD of apoptotic cells in each sample.

The alteration of lipid rafts on IL-4 deprivation was also analyzed in intact cells by confocal microscopy (Fig. 1C). Control IL-4-stimulated or IL-4-deprived cells for different times were incubated with FITC-labeled cholera toxin subunit B. We observed a homogeneous distribution of green fluorescence in the membrane of IL-4-stimulated cells. In contrast, we detected a nonhomogeneous distribution of fluorescence with interruption of the signal at the cell surface as well as a reduction in the fluorescence intensity, which proves that the rafts structure is already altered in 4-hour IL-4-deprived cells. Green fluorescence labeling on the cell surface progressively disappears as the IL-4 deprivation period increases. These confocal microscopy studies suggest an early alteration of lipid rafts in the course of apoptotic process.

Segregation of Bad from Lipid Rafts Is an Event Induced by IL-4 Deprivation

We have shown previously colocalization of a pool of Bad and lipid rafts in proliferating cells, whereas rafts were altered in apoptotic cells, and as a consequence, Bad translocates to mitochondria (13). To dissect whether alteration of rafts and, as a result, segregation of Bad is the first phenomenon occurring in the apoptotic process triggered by growth factor deprivation or vice versa, we analyzed the subcellular distribution of Bad in intact cells on distinct IL-4 deprivation periods (Fig. 2A). Immunofluorescence analyses show homogeneous distribution of Bad in plasma membrane and in the cytoplasm in both control and 4-hour IL-4-deprived cells. Interestingly, 8 hours on IL-4 withdrawal, we observed a decrease in the amount of Bad associated to the plasma membrane, reaching the minimum level 24 hours after lymphokine deprivation (Fig. 2A). The distribution of Bad was also analyzed by subcellular fractionation. Rafts and mitochondria were isolated from IL-4-stimulated or IL-4-deprived cells for different times. Bad was found to be associated to rafts in control IL-4-stimulated cells.

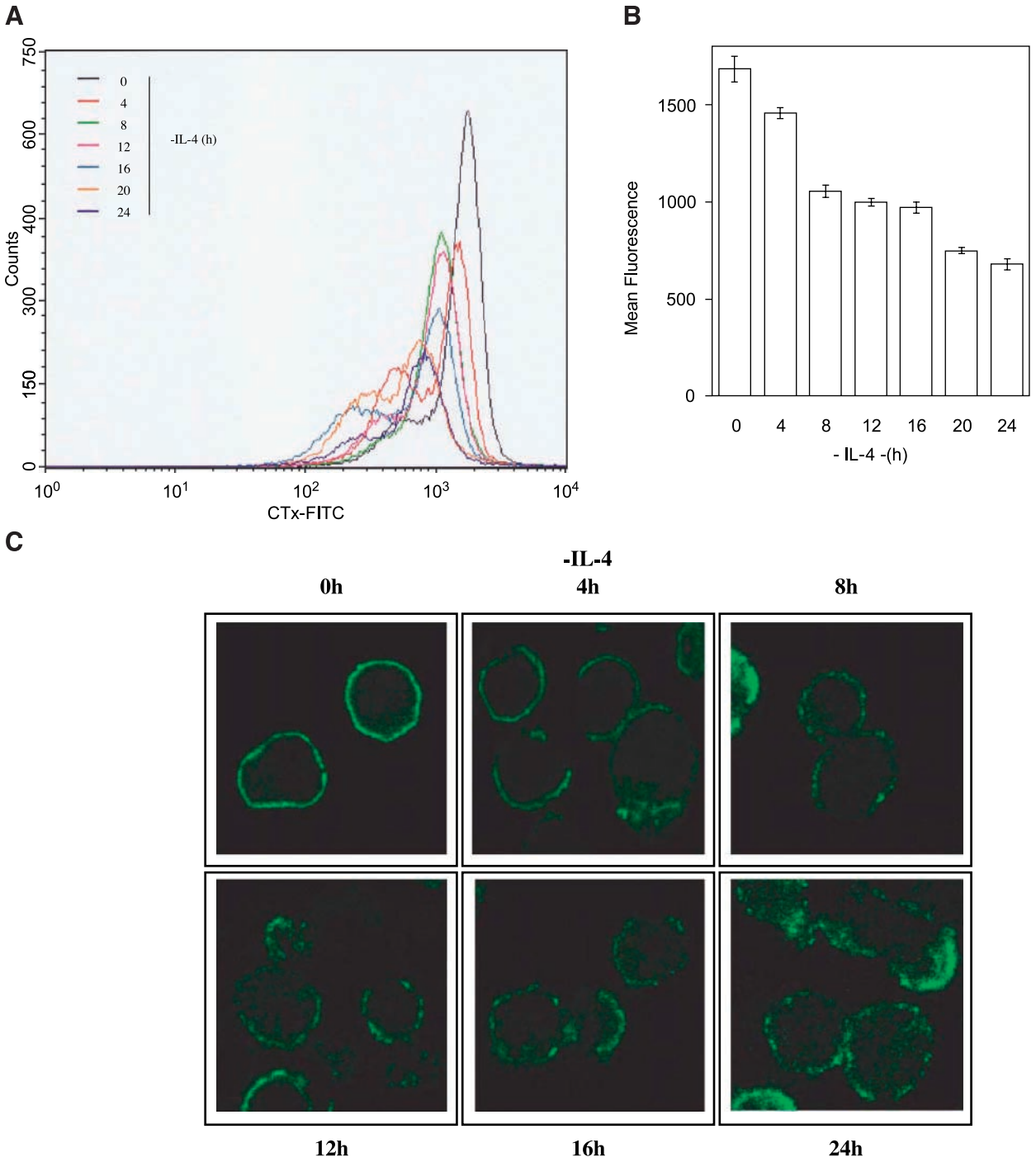

FIGURE 1. Effect of IL-4 deprivation on rafts staining. **A.** Cells were IL-4 stimulated or deprived for different times, stained with the rafts marker cholera toxin-FITC (*CTx-FITC*), which recognizes the ganglioside GM1, and analyzed by flow cytometry. Different lymphokine deprivation times are overlapped. Similar results of three independent experiments. **B.** Fluorescence of each analyzed sample. *Columns,* mean (n = 3); bars, SD. **C.** IL-4-stimulated or IL-4-deprived cells for different times were stained with cholera toxin-FITC and analyzed by confocal microscopy. Similar results of three independent experiments.

No difference in the quantity of attached Bad to rafts was detected 4 hours after IL-4 deprivation.The amount of Bad associated to rafts decreased on 8 hours of IL-4 starvation, and only traces of Bad were detected associated to rafts on 24 hours of IL-4 deprivation (Fig. 2B). In addition, the pool of Bad associated to rafts is dephosphorylated. To validate the fractionation protocol, rafts and the cytosolic fraction were immunoblotted with cholera toxin-biotin and α-tubulin antibody.

The subcellular localization of Bad was also examined in mitochondrial fraction of IL-4-stimulated or IL-4-deprived cells (Fig. 2C). Low amount of Bad was detected associated to mitochondrial fraction of both IL-4-stimulated and 4-hour IL-4-deprived cells. An increase in the amount of Bad localized to mitochondria was observed 8 hours after IL-4 deprivation, reaching the maximum 24 hours after lymphokine deprivation. At that time, only traces of Bad are associated to rafts (Fig. 2B). The purity of the mitochondrial and cytosolic fraction was confirmed by reimmunoblotting with α-VDAC and α-caspase-3 antibodies. Figure 2D shows that total Bad expression was not modified on IL-4 deprivation. Given that alteration of lipid rafts is detectable 4 hours after lymphokine deprivation, whereas Bad is still associated to lipid rafts, this result strongly suggests that alteration of rafts precedes Bad redistribution. Translocation of Bad to mitochondria was also confirmed in intact cells by confocal microscopy (Fig. 3). Double immunofluorescence analyses with anti-Bad and anti-mitochondria antibody show very weak association of Bad to mitochondria in IL-4-stimulated cells, whereas there is a significant fraction of Bad associated to mitochondria in 12-hour IL-4-deprived cells (Fig. 3).

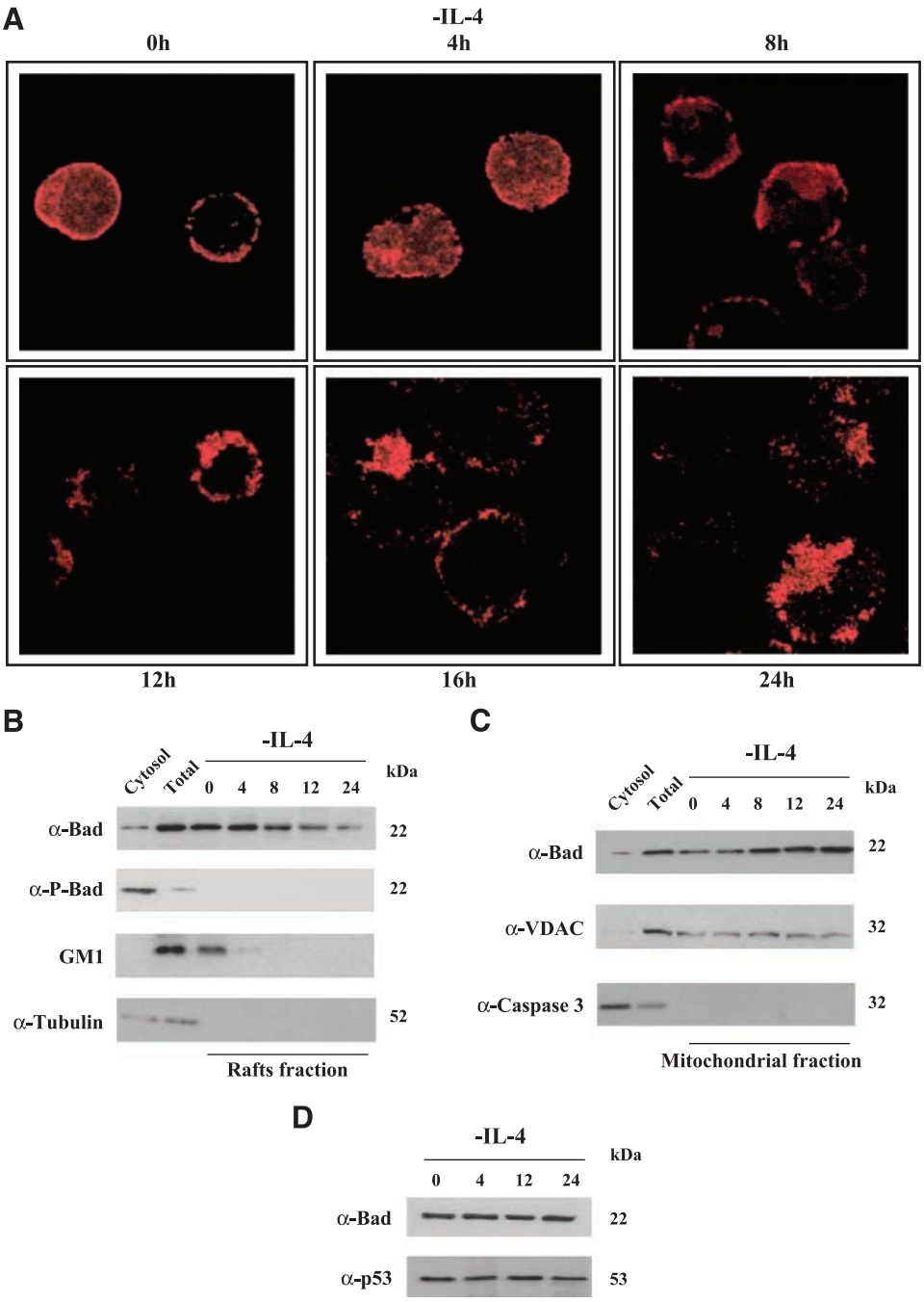

FIGURE 2. Bad redistribution on IL-4 withdrawal. **A.** IL-4-stimulated or IL-4-deprived cells were stained with anti-Bad antibody followed by Cy3-labeled secondary antibody and then analyzed by confocal microscopy. Similar results of three independent experiments. **B.** IL-4-stimulated or IL-4-deprived cells were Triton X-100 extracted and fractionated in Optiprep flotation gradient. Fractions were collected from the top to the bottom of the gradient. Only the insoluble fraction, representing rafts, is shown. Proteins were separated by SDS-PAGE, and the blot was hybridized with anti-Bad, anti-phospho-Bad, cholera toxin-biotin (rafts marker), and anti-tubulin (cytosolic marker). Total and cytosolic extracts were used as a control. **C.** Mitochondria were isolated from IL-4-stimulated or IL-4-deprived cells as described in Materials and Methods, separated by SDS-PAGE, and immunoblotted with anti-Bad, anti-VDAC (mitochondrial marker), and anti-caspase-3 (cytosolic marker). Total and cytosolic extracts were used as control. **D.** Cells were IL-4 stimulated or deprived for the indicated times and lysed. Total protein extracts were separated by SDS-PAGE, transferred to nitrocellulose, and probed with anti-Bad antibody. Protein bands were detected using enhanced chemiluminescence system. The blot was reprobed with anti-p53 as internal control of protein loading. Similar results of three independent experiments. Note molecular weight of the corresponding proteins.

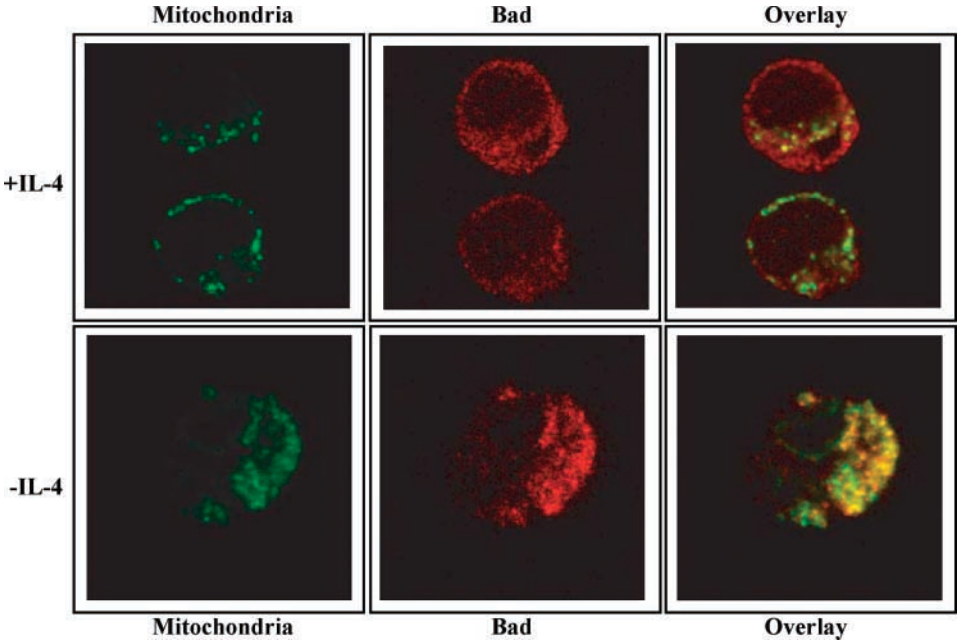

FIGURE 3. Mitochondrial localization of Bad. IL-4-stimulated or IL-4-deprived cells (12 hours) were stained with anti-Bad and anti-mitochondria antibody (Mito 2813) followed by Cy3- and Cy2-labeled secondary antibodies, respectively, and analyzed by confocal microscopy. Similar results of three independent experiments. Single confocal sections show fluorescence in *green* and *red*.

Because the integrity of lipid rafts is necessary for association of Bad, we analyzed whether other proteins known to be associated to rafts, such as Lck, are able to segregate on alteration of rafts. Rafts were isolated from IL-4-stimulated or IL-4-deprived cells and immunoblotted with anti-Lck antibody (Fig. 4). Lck was detected in the rafts fraction of control IL-4-stimulated and 4-hour IL-4-deprived cells, progressively decreasing on 8 hours of IL-4 deprivation. No Lck was detected on 12 hours of IL-4 starvation (Fig. 4), demonstrating that alteration of rafts induces segregation of attached proteins. Taken together, these results provide evidence that rafts alteration is an early event in the apoptotic process and its integrity is necessary for protein association.

Indirect Effect of IL-4 Deprivation on Rafts Alteration

We further examined whether the absence of IL-4 was responsible for rafts alteration or whether IL-4 deprivation gives an intracellular signal that triggers, as a final consequence, modification of rafts. For this purpose, IL-4-stimulated or IL-4-deprived cells for different times were treated with or without z-VAD-fmk to block caspase-dependent apoptosis and then incubated with cholera toxin-FITC followed by fluorescence-activated cell sorting analysis. As shown in Fig. 5A, we observed a significant diminution of the signal intensity with cholera toxin-FITC 4 hours after IL-4 deprivation. The level of staining progressively decreases as the IL-4 deprivation period increases (8 hours), confirming previous results (Fig. 1). Interestingly, z-VAD-fmk addition causes no reduction in signal intensity of the rafts marker cholera toxin-FITC on IL-4 deprivation (Fig. 5A), suggesting an indirect effect of IL-4 deprivation on rafts organization and that rafts alteration is dependent on caspase activation. To validate z-VAD-fmk action on the cells, apoptosis and caspase inhibition were analyzed. z-VAD-fmk treatment blocks caspase-9 activation and apoptosis in IL-4-deprived cells as shown in Fig. 5B and C. Nontreated cells show levels of apoptosis comparable with that shown in Table 1.

IL-4 Deprivation Induces Bad-Associated PP1α Phosphatase as Well as Caspase-9 and Caspase-3 Activation

We have shown previously that Bad is an *in vitro* and *in vivo* substrate for PP1α phosphatase and that growth factor deprivation–induced apoptosis operate by regulating cytoplasmic Bad dephosphorylation through PP1α phosphatase (13). Figure 6A shows phosphatase activity in cytoplasmic Bad immunoprecipitates of IL-4-stimulated or IL-4-deprived cells for different times. Phosphatase activity in the immunoprecipitates was measured using [^{32}P]phosphorylase *a* as substrate. Enzymatic activity was detected in Bad immunoprecipitates of IL-4-stimulated cells increasing 2 hours after IL-4 deprivation. The enzymatic activity progressively augments as the IL-4 deprivation period enlarges. No phosphatase activity was detected in control immunoprecipitates anti-c-Jun of IL-4-stimulated or IL-4-deprived cells. This result suggests that

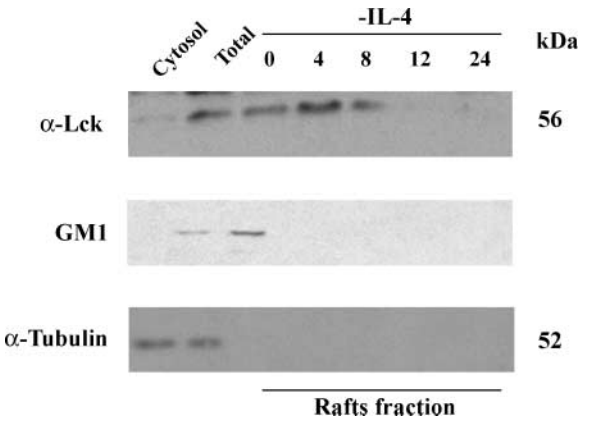

FIGURE 4. Subcellular localization of Lck in proliferating and apoptotic cells. Lipid rafts were isolated from IL-4-stimulated or IL-4-deprived cells in Optiprep flotation gradient. Proteins were separated by SDS-PAGE and immunoblotted with anti-Lck, cholera toxin-biotin, and anti-tubulin. Similar results of three independent experiments.

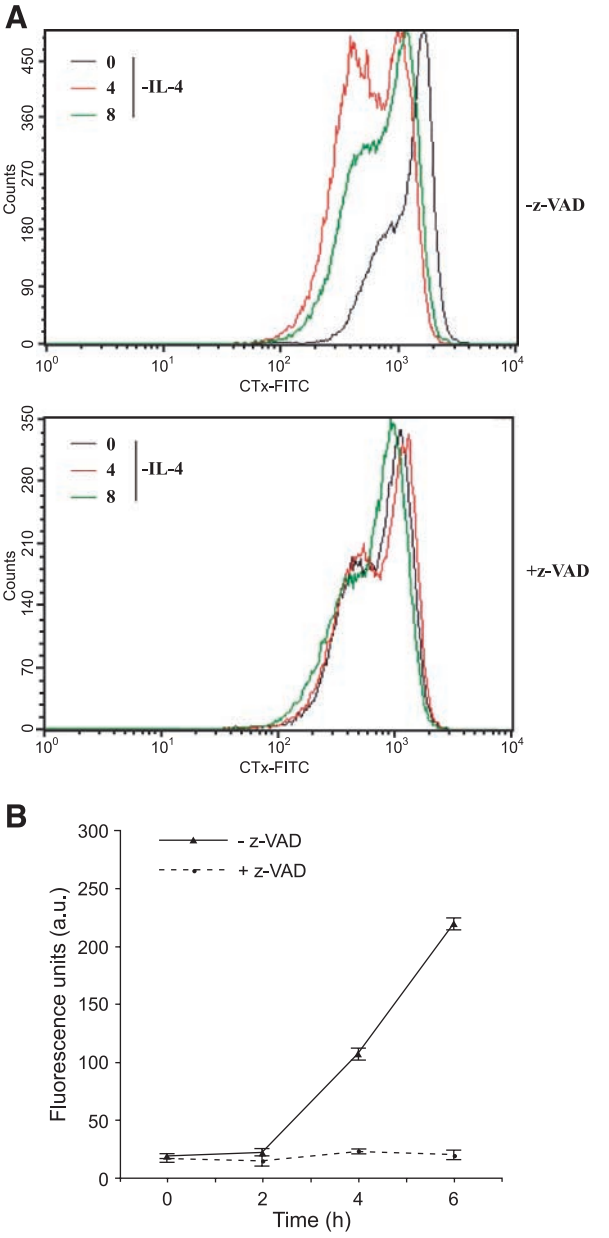

IL-4 deprivation rapidly induces Bad-associated phosphatase activation in a time-dependent manner. Figure 6B confirms that PP1α but not PP2A or PP2B was detected associated to Bad and was responsible for the enzymatic activity detected in cytoplasmic Bad immunoprecipitates. This association was also detected using radioimmunoprecipitation assay buffer (data not shown). Comparable PP1α levels were detected by Western blot in Bad immunoprecipitates from control IL-4-stimulted or IL-4-deprived cells. Reprobing the membrane with anti-Bad antibody showed similar levels of Bad in immunoprecipitates from control IL-4-stimulted or IL-4-deprived cells (Fig. 6B). This result suggests a rapid activation of PP1α phosphatase activity and, as a consequence, an immediate dephosphorylation of cytoplasmic Bad that turns Bad into a proapoptotic molecule.

We have shown previously that growth factor deprivation induces initiator caspase-9 as well as caspase-3 activation (14). To know whether caspase activation occurs upstream or downstream of Bad-associated PP1α phosphatase activation, we did kinetics of caspase-9 and caspase-3 activity on different periods of IL-4 deprivation. Figure 7A illustrates that caspase-9 and caspase-3 activation follow PP1α phosphatase activation, as the activity is detected 4 hours on IL-4 deprivation, progressively increasing with the deprivation kinetic (Fig. 7A). On the contrary, PP1α phosphatase activation was already detected 2 hours on IL-4 starvation. This result argues that caspase activation is a downstream event of PP1α phosphatase activation.

Caspase-9 and Caspase-3 Associate with Lipid Rafts in IL-4-Deprived Cells

It is known that localization of proteins to distinct subcellular compartments, including cellular membrane, is a critical event in multiple cellular pathways, such as apoptosis. Given that an increase in Bad-associated phosphatase activity is detected very early in the apoptotic process followed by caspase-9 and caspase-3 activation and that IL-4 deprivation is not directly responsible for rafts alteration, we wondered whether caspase-9 and caspase-3 could be localized and activated in lipid rafts on IL-4 starvation. For this purpose, we isolated rafts by Triton X-100 flotation gradient of control IL-4-stimulated or IL-4-deprived cells (Fig. 7B). Caspase-9 could not be detected in lipid rafts of IL-4-stimulated cells, progressively increasing during the starvation period, whereas pro-caspase-9 was only identified in lipid rafts of IL-4-stimulated and 4-hour IL-4-deprived cells. Both pro-caspase-9 and pro-caspase-3 were found in total extracts. Similarly, low level of caspase-3 was detected in rafts of control

FIGURE 5. Effect of caspase inhibition on rafts staining and apoptosis. **A.** Cells were IL-4 stimulated or deprived for different times in the presence or absence of the caspase inhibitor z-VAD-fmk. Cells were stained with the rafts marker cholera toxin-FITC and analyzed by flow cytometry. Results obtained from different times are overlapped. Mean fluorescence of each analyzed sample. Similar results of three independent experiments. **B.** TS1αβ cells were deprived of IL-4 for different times in the presence or absence of the caspase inhibitor z-VAD-fmk. Caspase-9 activity was determined in cytosolic extracts as fluorescence emission of the cleaved substrate. **C.** Cells were treated as in **B**, washed, stained with Annexin and propidium iodide, and then analyzed by flow cytometry. *Columns,* mean (n = 3); bars, SD.

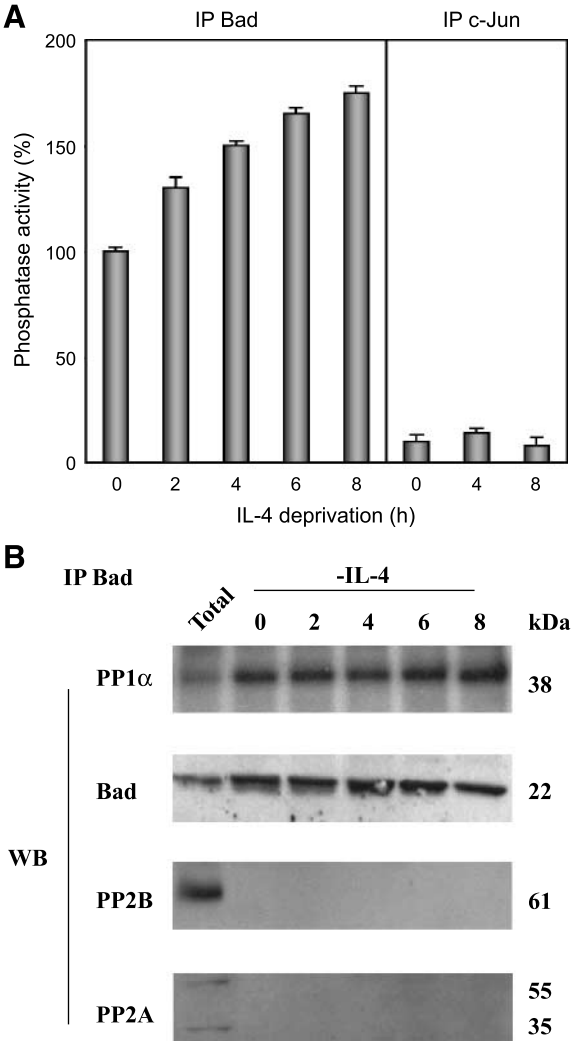

FIGURE 6. Estimation of PP1α phosphatase activity in Bad immunoprecipitates. **A.** Phosphatase activity was estimated in Bad immunoprecipitates from IL-4-stimulated or IL-4-deprived cells using [^{32}P]phosphorylase *a* as substrate. As a negative control, phosphatase activity was estimated in c-Jun immunoprecipitates. *Columns,* mean ($n = 3$); bars, SD. Phosphatase activity is percentage of the maximal activity detected in control IL-4-stimulated cells. **B.** Total extracts or cytoplasmic lysates from IL-4-stimulated or IL-4-deprived cells immunoprecipitated with anti-Bad were transferred to nitrocellulose and immunoblotted with PP1α. The blot was reprobed with anti-PP2A, anti-PP2B, and anti-Bad as internal controls. Molecular weight of the corresponding proteins. Representative of three independent experiments.

IL-4-stimulated cells, increasing as the starvation period enlarges. To validate the gradient procedure, the blot was hybridized with anti-Lck (rafts marker) and anti-Tim 23 (non-rafts marker).

Given that IL-4 deprivation firstly induces Bad-associated PP1α phosphatase activation and subsequently caspase-9 and caspase-3 activation, we asked whether PP1α activity was an upstream event in the rafts alteration cascade. We hypothesized that inhibition of PP1α phosphatase activity in IL-4-deprived cells may prevent caspase activation and apoptosis. For this purpose, we treated IL-4-stimulated or IL-4-deprived cells with the phosphatase inhibitor okadaic acid using a concentration affecting only PP1 (13). Figure 8A shows that IL-4-deprived cells treated with 1 μmol/L okadaic acid for 6 hours showed an inhibition of pro-caspase-9 and pro-caspase-3 activation as detected by Western blot. On the contrary, caspase-9 and caspase-3 activation were detected in nontreated IL-4-deprived cells. The effect of okadaic acid on PP1α phosphatase activity was determined by inhibition of Bad phosphorylation as described previously (13). Table 2 shows that IL-4-deprived cells treated with okadaic acid for 6 hours showed a significant reduction in the fraction of apoptotic cells (9%) compared with untreated cells (18%).

Taken together, these results strongly suggest that alteration of lipid rafts is the consequence of an intracellular signal delivered by IL-4 deprivation, which in turn triggers cytoplasmic Bad dephosphorylation via PP1α phosphatase followed by caspase-9 and caspase-3 activation. Caspases translocate to lipid rafts and promote rafts alteration probably due to its protease activity. As a consequence, Bad translocates from rafts to mitochondria, which correlates with apoptosis.

Discussion

Lipid rafts have been implicated in the regulation of numerous cellular events, including signal transduction (34), membrane traffic (35), and viral entry/infection (36). The large majority of these studies have relied on the detergent insolubility of lipid rafts for their purification. The most widely used detergent in these studies is Triton X-100, although other detergents have been used for this purpose, including CHAPS, Tween 20, Triton X-114, Lubrol, Brig 96, Brig 98, and sodium deoxycholate (37-40). Among all of them, Triton X-100 has the highest solubilization strength (41). Triton X-100-insoluble domains had a marker enrichment of sphingolipids and cholesterol relative to glycerophospholipids. Lipid composition can vary in distinct protein-containing rafts, and detergent insolubility may be used as a basis to separate distinct types of rafts.

We have shown that Bad function is regulated by dynamic interaction with lipid rafts or mitochondria (13). The distinct Bad distribution and function are directly related to IL-4 stimulation or deprivation of the cells. This is in agreement with recent results showing that association of proteins to lipid rafts can be modulated because some proteins may be excluded from rafts by association with other proteins (42).

As early as 4 hours after lymphokine deprivation, we are able to observe apoptosis and alteration of rafts as detected by

Table 2. Effect of Okadaic Acid on Apoptosis

Apoptotic Cells (%)			
Time (h)	IL-4	Okadaic Acid	Apoptosis
0	+	−	3 ± 2
6	−	+	9 ± 1
0	+	+	5 ± 3
6	−	−	18 ± 3

NOTE: Cells were treated for 6 hours with or without 1 μmol/L okadaic acid in the presence or absence of IL-4. Cells were washed, stained with Annexin and propidium iodide, and analyzed by flow cytometry. SD for $n = 3$.

fluorescence-activated cell sorting and confocal microscopy, respectively. On the contrary, at that time, we did not observe significant modification of Bad staining. Subcellular fractionation studies confirm the presence of Bad associated to lipid rafts in control IL-4-stimulated or 4-hour IL-4-deprived cells. In fact, rafts alteration seems to be a consequence of an intracellular signal triggered by IL-4 deprivation. Growth factor deprivation induces Bad-associated PP1α activation, which dephosphorylates cytoplasmic Bad, activating caspase-9 and caspase-3. As a consequence, the Bad pool associated to rafts translocates toward the mitochondria leading to apoptotic cell death. This result strongly suggests that segregation of Bad from rafts 8 hours after IL-4 deprivation is a consequence of preceding apoptotic signals triggered by IL-4 withdrawal. Thus, translocation of Bad from rafts to mitochondria is observed in advanced stages of growth factor deprivation.

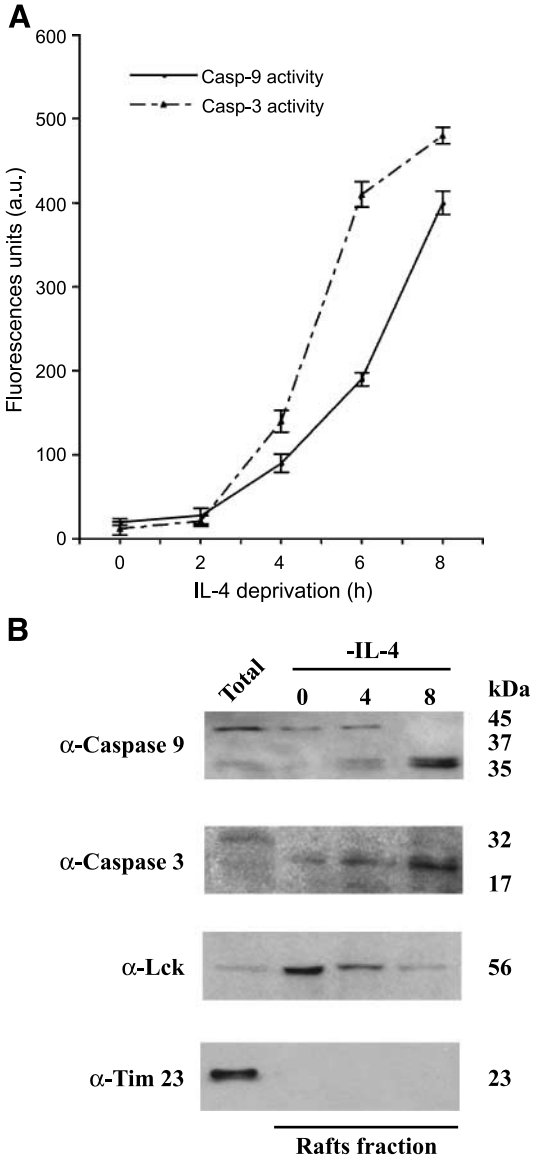

FIGURE 7. Influence of IL-4 deprivation on caspase activity and localization. **A.** Cells were cultured in the presence or absence of IL-4 for the indicated times. Caspase-9 and caspase-3 activity was determined in cytosolic extracts as fluorescence emission of the cleaved substrates. *Columns,* mean ($n = 3$); bars, SD. **B.** IL-4-stimulated or IL-4-deprived cells were Triton X-100 extracted and fractionated in Optiprep flotation gradient. Only the insoluble proteins are shown. Immunoblot was probed with anti-caspase-9 and anti-caspase-3. As internal control, the blot was hybridized with anti-Lck (rafts marker) and anti-Tim 23 (non-rafts marker). Similar results of three independent experiments. Molecular weights of the corresponding proteins.

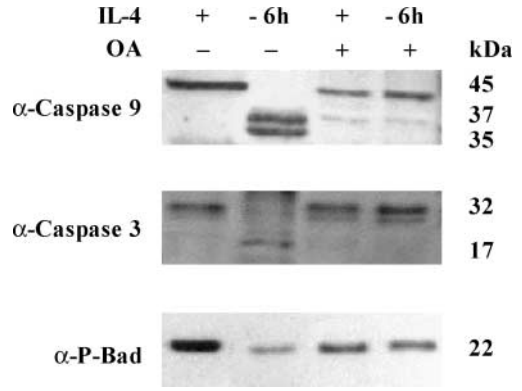

FIGURE 8. Effect of the phosphatase inhibitor okadaic acid on caspase-9 and caspase-3 activity and apoptosis. **A.** IL-4-stimulated or IL-4-deprived cells were treated with 1 μmol/L okadaic acid (*OA*) for 6 hours. Total extracts were transferred to nitrocellulose. The membrane was probed with anti-caspase-9, anti-caspase-3, and anti-phospho-Bad, the latter to verify that okadaic acid treatment *in vivo* blocked PP1α phosphatase activity. Molecular weight of the corresponding proteins. Protein bands were detected using enhanced chemiluminescence. Similar results were obtained in two independent experiments.

Our findings clearly show that rafts alteration represents an early event in the apoptotic process induced by IL-4 deprivation. The following question to answer was to know whether this phenomenon was a direct or indirect effect of IL-4. Blocking apoptosis via caspase inhibition strongly suggests an indirect effect of IL-4 in rafts alteration, indicating that IL-4 deprivation triggers an intracellular signal that induces initially Bad-associated PP1α phosphatase activation and subsequently caspase-9 and caspase-3 activation. It is interesting to notice the presence of two different pools of Bad: the cytoplasmic pool, which is phosphorylated, and the pool of Bad attached to rafts, which is dephosphorylated (22). The IL-4 deprivation-triggered pathway starts with the dephosphorylation of cytoplasmic Bad by PP1α, whereas the pool of Bad sequestered in rafts is already dephosphorylated. This association may be involved in steps leading to Bad inactivation because rafts do not constitute the final site of activation. This indirect effect of IL-4 withdrawal can be considered as a model for amplification of the cytoplasmic Bad dephosphorylation effect because dephosphorylation triggers its proapoptotic role and, as a consequence, the execution of the apoptotic signaling cascade: activation of caspases, segregation of Bad from rafts, and translocation to mitochondria, thus amplifying apoptotic cell death. In addition, inhibition of PP1α phosphatase or caspase activation blocks apoptosis and alteration of rafts, reinforcing our hypothesis.

It has recently been shown that in CD4 T cells the death-inducing signaling complex, Fas-associated death domain protein, and pro-caspase-8 are recruited to lipid rafts in Fas-induced apoptosis in CD4 T cells (43, 44).

Moreover, the anticancer drug resveratrol induces the redistribution of Fas receptor in membrane rafts of colon carcinoma cells (26). Similar observation has been made recently in human leukemic cells exposed to the antitumor ether lipid edelfosine (21). This translocation of Fas into membrane rafts may provide a mechanism for amplifying Fas signaling through reorganization of membrane microdomains, involving rafts in cancer chemotherapy and Fas-mediated apoptosis. In addition to Fas, it has been shown that other apoptotic molecules are recruited into lipid rafts: Fas-associated death domain protein, pro-caspase-8, pro-caspase-10, c-Jun NH_2-terminal kinase, and Bid. This molecular aggregation may link Fas and mitochondrial signaling pathways (24). Other signaling molecules, such as Akt2, phosphatidylinositol 3′-kinase, protein kinase C, PTEN, CD28, and Lck, have also been detected in lipid rafts.

Here, we have shown that rafts alteration is a consequence of an early intracellular signal triggered by IL-4 deprivation. Even if our results confirm the pivotal role of rafts in the control of apoptosis as illustrated in the model presented in Fig. 9, activation arrow; , translocation arrow, we do not exclude the possibility that IL-4 deprivation might induce changes in lipid rafts composition. According to this, it has been shown recently that ceramide can displace cholesterol from rafts using artificial lipid vesicles containing coexisting rafts domains and disordered fluid domains (18).

Materials and Methods

Cells, Lymphokines, and Reagents

Murine T cell line TS1αβ can be independently propagated in IL-2, IL-4, or IL-9 (45). Murine recombinant IL-4 or supernatant of a HeLa subline transfected with pKCRIL-4-neo was used as a source of murine IL-4. Okadaic acid, FITC-labeled cholera toxin subunit B, Optiprep, and cholera toxin-biotin were from Sigma-Aldrich (St. Louis, MO). Vectashield was from Vector Laboratories (Burlingame, CA). Anti-Bad, anti-phospho-Bad (Ser^{112}, Ser^{136}, and Ser^{155}), and anti-PP1α antibodies were from Calbiochem (La Jolla, CA), Cell Signaling (Beverly, MA), New England Biolabs (Beverly, MA), and Transduction Laboratories (Lexington, KY). Anti-Tim 23, anti-PP2B, anti-p53, anti-caspase-3, and anti-Lck were from Transduction Laboratories. Cy2- and Cy3-conjugated secondary antibodies were purchased from Molecular Probes (Eugene, OR). Anti-VDAC antibody was from PharMingen

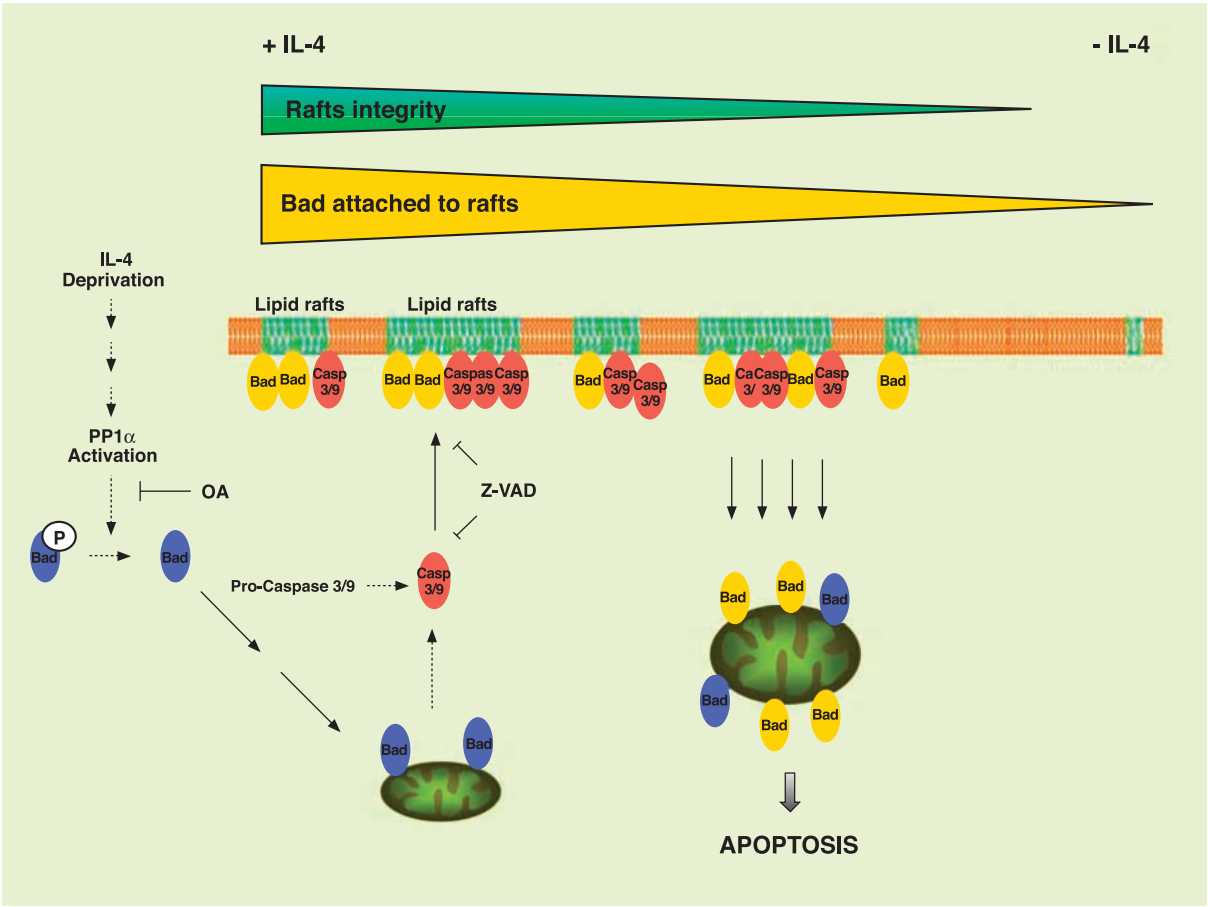

FIGURE 9. Schematic model for amplification of cytoplasmic Bad dephosphorylation effect. IL-4 deprivation induces PP1α phosphatase activity, which in turn dephosphorylates cytoplasmic Bad. Dephosphorylated Bad translocates to mitochondria followed by induction of caspase-9 and caspase-3 activation. Proteases migrate to rafts causing its alteration, and as a consequence, the Bad pool attached to the rafts translocates to mitochondria, thus amplifying the apoptotic response. The final consequence of the pathway triggered by IL-4 withdrawal is the apoptotic death of the cell.

(San Diego, CA). Anti-mitochondria serum (Mito 2813: α-pyruvate dehydrogenase) was a gift from Dr. A. Serrano (Centro Nacional de Biotecnologia, Madrid, Spain). Anti-caspase-9 was from MBL (Nagoya, Japan), and anti-c-Jun antibody was from Santa Cruz Biotechnology (Santa Cruz, CA). Protease and phosphatase inhibitor cocktails were obtained from Sigma-Aldrich, and caspase inhibitor z-VAD-fmk was from Bachem (Bubendorf, Switzerland). Anti-PP2A was generated at Pierre et Marie Curie University (Paris, France). Peroxidase-conjugated goat anti-rabbit and anti-mouse immunoglobulin antibody were from DAKO (Glostrup, Denmark). Enhanced chemiluminescence was from Amersham (Buckinghamshire, United Kingdom), and the Annexin kit was from Immunotech (Marseilles, France).

Cell Cycle Analysis and Cholera Toxin-FITC Labeling

A total of 2.5×10^5 TS1αβ cells were IL-4-stimulated or IL-4-deprived for different times and washed with ice-cold PBS diluted in ice-cold binding buffer as well as stained with Annexin and propidium iodide. Samples were maintained on ice for 10 minutes in the dark and then analyzed by flow cytometry. Apoptosis was measured as the percentage of cells in the sub-G_1 region of the fluorescence scale having a hypodiploid DNA content. For cholera toxin-FITC labeling, IL-4-stimulated or IL-4-deprived cells were washed with chilled PBS and fixed for 5 minutes on ice with 1% paraformaldehyde. Cells were washed with PBS-bovine serum albumin and then incubated with cholera toxin-FITC (20 minutes, 6 μg/mL). After washing with PBS-bovine serum albumin, cells were analyzed by flow cytometry. Alternatively, cells were permeabilized for 2 minutes with 0.1% saponin in PBS and incubated with anti-Bad and/or anti-mitochondria antibody for 1 hour in PBS-bovine serum albumin followed by Cy3- and/or Cy2-labeled secondary antibody for 1 hour. After several washing steps, cells were incubated with methanol for 10 minutes at −20°C, mounted with Vectashield medium, and analyzed by confocal microscopy.

Immunoprecipitation and Western Blot

Cells (1×10^7) were IL-4 stimulated or deprived and lysed for 20 minutes at 4°C in lysis buffer [50 mmol/L Tris-HCl (pH 8), 1% NP40, 137 mmol/L NaCl, 1 mmol/L $MgCl_2$, 1 mmol/L $CaCl_2$, 10% glycerol, protease and phosphatase inhibitor mixture]. Alternatively, radioimmunoprecipitation assay buffer has been used for cell lysis. Lysates were immunoprecipitated with the corresponding antibody. Protein A-Sepharose was added for 1 hour at 4°C, and after washing, immunoprecipitates were lysed in Laemmli sample buffer. Protein extracts were separated by SDS-PAGE, transferred to nitrocellulose, blocked with 5% nonfat dry milk in TBS [20 mmol/L Tris-HCl (pH 7.5), 150 mmol/L NaCl], and incubated with the primary antibody in TBS-0.5% nonfat dry milk. Membranes were washed with TBS-0.05% Tween 20 and incubated with peroxidase-conjugated secondary antibody. After washing, membranes were developed using enhanced chemiluminescence system.

Isolation of Mitochondria and S-100 Fraction

Mitochondria were isolated using a modification of the method described by Yang et al. (46). Briefly, 20×10^6 cells were IL-4 stimulated or deprived, harvested, and washed with chilled PBS. Cell pellet was resuspended in 5 volumes of ice-cold buffer A [20 mmol/L HEPES-KOH (pH 7.5), 10 mmol/L KCl, 1.5 mmol/L $MgCl_2$, 1 mmol/L EDTA, 1 mmol/L EGTA, 1 mmol/L DTT, 0.1 mmol/L phenylmethylsulfonyl fluoride, 250 mmol/L sucrose] supplemented with protease inhibitors. Cells were disrupted in a Dounce homogenizer, the nuclei were centrifuged ($1{,}000 \times g$, 10 minutes, 4°C), and the supernatant was further centrifuged ($1{,}000 \times g$, 15 minutes, 4°C). The extracted mitochondrial pellet was resuspended in buffer A and stored at −80°C. The supernatant was centrifuged ($100{,}000 \times g$, 1 hour, 4°C), and the resulting S-100 fraction stored at −80°C.

Triton X-100 Flotation

IL-4-stimulated or IL-4-deprived cells were lysed in TXNE buffer [50 mmol/L Tris-HCl (pH 7.4), 150 mmol/L NaCl, 5 mmol/L EDTA, 2% Triton X-100] containing protease inhibitor mixture. Detergent-insoluble membranes were isolated by ultracentrifugation ($17{,}000 \times g$, 4 hours, 4°C) in a 30% to 35% gradient of Optiprep as described previously (47, 22).

Enzyme Assay for Caspase Activity

Cells were washed with ice-cold PBS and resuspended in extraction buffer [50 mmol/L Tris-HCl (pH 7.6), 150 mmol/L NaCl, 0.5 mmol/L EDTA, 10 mmol/L NaH_2PO_4, 10 mmol/L Na_2HPO_4, 1% NP40, 0.4 mmol/L Na_3V0_4, 1 mmol/L phenylmethylsulfonyl fluoride, protease inhibitor cocktail]. Cell lysate was centrifuged ($20{,}000 \times g$, 30 minutes, 4°C), and proteins (5 μg) diluted in assay buffer [25 mmol/L HEPES (pH 7.5), 0.1 mmol/L CHAPS, 10% sucrose, 10 mmol/L DTT, 0.1 mg/mL ovalbumin] were incubated with fluorescent substrate sequence for caspase-9 and caspase-3. Cleaved substrate fluorescence was determined by reverse-phase HPLC.

In vitro *Phosphatase Assay*

Cells were lysed in lysis buffer, and supernatanys were immunoprecipitated (2 hours, 20°C) with anti-Bad antibody and incubated with protein A-Sepharose beads (45 minutes, room temperature). Immunoprecipitates were washed with phosphatase buffer [50 mmol/L Tris-HCl (pH 7.5), 0.1% 2-mercaptoethanol, 0.1 mmol/L EDTA, 1 mg/mL bovine serum albumin], mixed with [^{32}P]phosphorylase *a*, and diluted in phosphatase buffer supplemented with 4 mmol/L caffeine. The reaction was incubated for 40 minutes at 30°C and stopped by adding 200 μL of 20% trichloroacetic acid followed by centrifugation. A total of 185 μL were used to estimate the generation of free phosphate liberated from [^{32}P]phosphorylase *a*.

References

1. Kerr JF, Willy AH, Currie AR. Apoptosis, a basic biological phenomenon with wide-ranging implications in tissue kinetics. Br J Cancer 1972;26:239–57.

2. Jacobson MD, Weil M, Raff MC. Programmed cell death in animal development. Cell 1997;88:347–54.

3. Strasser A, O'Connor L, Dixit VM. Apoptosis signalling. Annu Rev Biochem 2000;69:217–45.

4. Reed JC. Apoptosis-regulating proteins as targets for drug discover. Trends Mol Med 2001;7:314–9.

5. Gross A, McDonnell JM, Korsmeyer SJ. Bcl-2 family members and the mitochondria in apoptosis. Genes Dev 1999;13:1899–911.

6. Fleischer A, Rebollo A, Ayllon V. BH3-only proteins: the lords of death. Arch Immunol Ther Exp 2003;51:9–17.

7. Kremmer E, Ohst K, Kiefer J, Brewis N, Walter G. Separation of PP2A core enzyme and holoenzyme with monoclonal antibodies against the regulatory A subunit: abundant expression of both forms in T cells. Mol Cell Biol 1997;17: 1692–701.

8. Hubbard MJ, Cohen P. On target with new mechanism for the regulation of protein phosphorylation. Trends Biochem Sci 1993;18:172–7.

9. Faux MC, Scott JD. More on targeting with protein phosphorylation: conferring specificity by location. Trends Biochem Sci 1996;21:312–5.

10. Cohen P, Klumpp S, Schelling DL. An improved procedure for identifying and quantitating protein phosphatases in mammalian tissues. FEBS Lett 1989;250:596–600.

11. Cohen P, Holmes CF, Tsukitani Y. Okadaic acid: a new probe for the study of cellular regulation. Trends Biochem Sci 1990;15:98–102.

12. Favre B, Turoski P, Hemmings BA. Differential inhibition and modification of PP1 and PP2A in MCF7 cells treated with calyculin, okadaic acid and tautomycin. J Biol Chem 1997;272:13856–63.

13. Ayllon V, Martinez-A C, Garcia A, Cayla X, Rebollo A. PPα is a Ras-activated Bad phosphatase that regulates IL-2 deprivation induced apoptosis. EMBO J 2000;19:2237–46.

14. Fleischer A, Ayllon V, Rebollo A. ITM2Bs regulates apoptosis by inducing loss of mitochondrial membrane potential. Eur J Immunol 2002; 32:3498–505.

15. Brown DA, London E. Functions of lipid rafts in biological membranes. Annu Rev Cell Dev Biol 1998;14:111–36.

16. Kabouridis P, Janzen J, Magee L, Ley CS. Cholesterol depletion disrupts lipid rafts and modulates the activity of multiple signalling pathways. Eur J Immunol 2000;30:954–61.

17. Meer G, Lisman Q. Sphingolipid transport: rafts and translocators. J Biol Chem 2002;277:25855–9.

18. London M, London E. Ceramide selectively displaces cholesterol from ordered lipid domains (rafts): implications for lipid rafts structure and function. J Biol Chem 2004;279:9997–10004.

19. Harder T, Scheiffele P, Verdake P, Simons K. Lipid domain structure of the plasma membrane revealed by patching of membrane components. J Cell Biol 1998;141:929–42.

20. Gajate C, Fonteriz RI, Cabaner C, et al. Intracellular triggering of Fas, independently of FasL, as a new mechanism of antitumor ether lipid-induced apoptosis. Int J Cancer 2000;85:674–82.

21. Gajate C, Mollinedo F. The antitumor ether lipid ST-18-OCH(3) induces apoptosis through translocation and capping of Fas/CD95 into membrane rafts in human leukemic cells. Blood 2001;98:3860–3.

22. Ayllon V, Fleischer A, Cayla X, Garcia A, Rebollo A. Segregation of Bad from lipid rafts is implicated in the induction of apoptosis. J Immunol 2002; 168:3387–93.

23. Gajate C, Mollinedo F. Biological activities, mechanisms of action and biomedical prospect of edelfosine, a proapoptotic agent in tumor cells. Curr Drug Metab 2002;2:491–525.

24. Gajate C, Del Canto-Janez E, Acuna AU, et al. Intracellular triggering of Fas aggregation and recruitment of apoptotic molecules into Fas-enriched rafts in selective tumor apoptosis. J Exp Med 2004;200:356–65.

25. Aouad SM, Cohen LY, Sharif-Askari E, Haddad EK, Alam A, Sekaly RP. Caspase-3 is a component of Fas death-inducing signaling complex in lipid rafts and its activity is required for complete caspase-8 activation during Fas-mediated cell death. J Immunol 2004;172:2316–23.

26. Delmas D, Rebe C, Lacour S, et al. Resveratrol-induced apoptosis is associated with Fas redistribution in the rafts and the formation of a death inducing signalling complex in colon cancer cells. J Biol Chem 2003;278: 41482–90.

27. Li X, Leu S, Cheong A, et al. Akt2, phosphatidylinositol 3-kinase, and PTEN are in lipid rafts of intestinal cells: role in absorption and differentiation. Gastroenterology 2004;126:122–35.

28. Bauer B, Jenny M, Fresser F, Uberall F, Baier G. AKT1/PKBα is recruited to lipid rafts and activated downstream of PKC isotypes in CD3-induced T cell signaling. FEBS Lett 2003;54:155–62.

29. Legler DF, Micheau O, Doucey MA, Tschopp J, Bron C. Recruitment of TNF receptor 1 to lipid rafts is essential for TNFα-mediated NF-κB activation. Immunity 2003;5:655–64.

30. Vamosi G, Bodnar A, Vereb G, et al. IL-2 and IL-15 receptor α-subunits are coexpressed in a supramolecular receptor cluster in lipid rafts of T cells. Proc Natl Acad Sci U S A 2004;101:11082–7.

31. Filipp D, Zhang J, Leung BL, et al. Regulation of Fyn through translocation of activated Lck into lipid rafts. J Exp Med 2003;197:1221–7.

32. Sadra A, Cinek T, Imboden JB. Translocation of CD28 to lipid rafts and costimulation of IL-2. Proc Natl Acad Sci U S A 2004;101:11422–7.

33. Garcia A, Cayla X, Fleischer A, et al. Rafts, a simply way to control apoptosis by subcellular redistribution. Biochimie 2003;85:727–31.

34. Simons K, Toomre D. Lipid rafts and signal transduction. Nat Rev Mol Cell Biol 2000;1:31–9.

35. Ikonen E. Roles of lipid rafts in membrane transport. Curr Opin Cell Biol 2001;4:470–7.

36. Chazal N, Gerlier D. Virus entry, assembly, budding, and membrane rafts. Microbiol Mol Biol Rev 2003;2:226–37.

37. Brown DA, Rose JK. Sorting of GPI-anchored proteins to glycolipid-enriched membrane subdomains during transport to the apical cell surface. Cell 1992;68:533–44.

38. Madore N, Smith KL, Graham CH, et al. Functionally different GPI proteins are organized in different domains on the neuronal surface. EMBO J 1999;24:6917–26.

39. Roper K, Corbeil D, Huttner WB. Retention of prominin in microvilli reveals distinct cholesterol-based lipid micro-domains in the apical plasma membrane. Nat Cell Biol 2000;2:582–92.

40. Drevot P, Langlet C, Guo XJ, et al. TCR signal initiation machinery is pre-assembled and activated in a subset of membrane rafts. EMBO J 2002;8: 1899–908.

41. Schuck S, Honsho M, Ekroos K, Shevchenko A, Simons K. Resistance of cell membranes to different detergents. Proc Natl Acad Sci U S A 2003;100: 5795–800.

42. Field K, Holowka D, Baird B. Fc epsilon RI-mediated recruitment of p53/p56lyn to detergent resistant membrane domains accompanies cellular signalling. Proc Natl Acad Sci U S A 1995;92:9201–12.

43. Hueber AO, Bernard AM, Herincs Z, Couzinet A, He HT. An essential role for membrane rafts in the initiation of Fas-triggered cell death in mouse thymocytes. EMBO Rep 2002;3:190–6.

44. Scheel-Toellner D, Wang K, Singh R, Majeed S, Raza K, Curnow SJ, Salmon M, Lord JM. The death-inducing signalling complex is recruited to lipid rafts in Fas-induced apoptosis. Biochem Biophys Res Commun 2002;297: 876–9.

45. Pitton C, Rebollo A, Van Snick J, Theze J, Garcia A. High affinity and intermediate affinity forms of the IL-2R expressed in an IL-9-dependent murine T cell line deliver proliferative signals via differences in their transduction pathways. Cytokine 1993;5:362–9.

46. Yang J, Liu X, Bhalla K, et al. Prevention of apoptosis by Bcl-2: release of cytochrome *c* from mitochondria. Science 1997;275:1129–37.

47. Mañes S, Mira E, Gomez-Mouton C, et al. Membrane raft microdomains mediate front-rear polarity in migrating cells. EMBO J 1999;18:6211–20.